

AperTO - Archivio Istituzionale Open Access dell'Università di Torino

**Electron paramagnetic resonance study of vanadium exchanged H-ZSM5 prepared by vapor reaction of VCl<sub>4</sub>. The role of <sup>17</sup>O isotope labelling in the characterisation of the metal oxide interaction**

**This is a pre print version of the following article:**

*Original Citation:*

*Availability:*

This version is available <http://hdl.handle.net/2318/1765159> since 2020-12-24T17:37:05Z

*Published version:*

DOI:10.1016/j.jcat.2020.06.029

*Terms of use:*

Open Access

Anyone can freely access the full text of works made available as "Open Access". Works made available under a Creative Commons license can be used according to the terms and conditions of said license. Use of all other works requires consent of the right holder (author or publisher) if not exempted from copyright protection by the applicable law.

(Article begins on next page)

# Electron Paramagnetic Resonance Study of Vanadium Exchanged H-ZSM5 Prepared by Vapor Reaction of $\text{VCl}_4$ . The role of $^{17}\text{O}$ Isotope Labelling in the Characterisation of the Metal Oxide Interaction.

Valeria Lagostina, Enrico Salvadori, Mario Chiesa, Elio Giamello

*Department of Chemistry University of Torino, Via Giuria, 9 10125 – Torino, Italy.*

## Abstract

Site isolated vanadium ions supported on zeolites are central in many catalytic processes. However, an atomistic description of the species formed is often hampered by the heterogeneous nature of zeolites and the random distribution of active species. In this contribution we applied pulsed electron paramagnetic resonance spectroscopy on  $^{17}\text{O}$  exchanged ZSM-5 zeolite loaded with V(IV) ions, via gas phase reaction with  $\text{VCl}_4$  vapors. From the magnetic parameters relative to  $^1\text{H}$ ,  $^{17}\text{O}$ ,  $^{27}\text{Al}$  and  $^{51}\text{V}$  isotopes we prove that a single, structurally well-defined  $\text{VO}(\text{OH})^+$  species is formed at zeolite Al framework sites and derive a detailed atomistic model inclusive of bond lengths and angles. Comparison is set to vanadyl aquo complexes, highlighting analogies between surface and solution coordination chemistry. The results showcases the power of EPR spectroscopy and  $^{17}\text{O}$  isotopic labelling in the geometrical and electronic characterisation of inorganic complexes formed at the surface of oxide materials. Pulsed EPR on disorder systems can therefore compete in structural insight with more well-established X-ray techniques.

## Introduction

Supported metal oxide catalysts, where metal ions or atoms are anchored on the surface of oxide materials represent an evergreen subject of interest due to their practical applications in a vast range of industrially relevant catalytic reactions. Efforts from both academic and industrial sides are placed to understand and control the structural features and the nature of the chemical bonding between the metal and the surface, as both have a significant impact on the catalyst performance.

The interaction of transition metal ions (TMIs) with oxide surfaces bears resemblance to solution and solid state coordination chemistry, an analogy that led M. Che to develop the notion of the so-called interfacial coordination chemistry (ICC).[1] The concepts of solution coordination chemistry can provide a useful framework to describe solid state systems, where transition metal ions, usually the active catalytic species, interact with the surface of an oxide support, which can be treated as a macroligand. In this way critical parameters related to the electronic and geometrical structure of the supported TMI that ultimately determine the catalytic properties, can be rationalized with reference to molecular systems.

Fortunately enough, TMIs on oxide surfaces are usually the catalytic active sites, representing, as repeatedly suggested by Che,[2] an ideal target for spectroscopic investigations aimed at elucidating

their local environment and the changes in the electronic structure brought about by the interaction with surface. One critical aspect in this context are the electronic effects exerted by the oxide surface on deposited TMIs, effects which depend on the chemical nature of the support (i.e. acid-base properties, electronegativity, reducibility) and on its topological features (i.e. local coordination, morphology etc.) All these features impact the nature of the chemical bonding between the surface and the TMI and can be explored by a number of spectroscopic techniques, using the TMI itself as a convenient probe. Due to the partially filled *d* orbitals and their sensitivity to the first and even successive ligand spheres, magnetic and optical properties of surface bound TMIs are particularly well suited to report on even subtle changes in the local coordination environment. Among different spectroscopic methods due to its selectivity to open-shell electronic configurations and its sensitivity, Electron Paramagnetic Resonance (EPR) spectroscopy is a unique tool for the determination of the structure and reactivity of TMIs on oxide materials at the atomistic level. **[Errore. Il segnalibro non è definito.,3]** EPR is a spectroscopic technique that allows detection of paramagnetic centres and their coupled magnetic nuclei with spatial resolution from the atomic up to the nanometer scale. EPR spectroscopy has been abundantly used as a key spectroscopic tool to reveal structural details of open-shell metal atoms, ions, molecules and molecular ions in oxide systems. At first, only conventional Continuous Wave (CW-) EPR was used where information was limited to the *g* values and hyperfine couplings related to the paramagnetic centre. Hyperfine couplings (related to the interaction between the electron spin and the nuclear spin of atoms in contact with the unpaired electron) are the critical parameters to derive information on the electron spin density distribution in a given system. CW-EPR of polycrystalline powders limits the investigation of the hyperfine coupling to the nucleus of the paramagnet itself or, provided the interaction is strong enough, to nuclei in the first coordination sphere around it. However, following the rapid technological and methodological developments in the field of EPR started in the 1990's, the EPR toolbox has expanded enormously incorporating so called hyperfine techniques, which can provide sub-MHz resolution, allowing to couple the sensitivity and selectivity of EPR with the resolution of NMR. In this way coordination spheres up to the third can be investigated monitoring the delocalization of the electronic wavefunction and the configuration of the surrounding nuclei; a direct reflection of the nature of the chemical bond.

Considering the metal atom-oxide interaction, it is evident that the possibility to directly monitor the electron spin density delocalization from the TMI to the oxide ions of the support offers an invaluable tool for a full description of the metal-oxide chemical interaction. However, the natural abundance of the only magnetically active oxygen isotope ( $^{17}\text{O}$   $I = 5/2$   $ab=0.037\%$ ) is by far too low to detect a hyperfine structure, thus  $^{17}\text{O}$  isotopic enrichment strategies are needed.

The use of  $^{17}\text{O}$  labelling of oxide systems is relatively common in NMR spectroscopy [4] but far less practiced in the case of EPR, largely because advanced hyperfine techniques are usually needed for the detection of relatively small hyperfine couplings. M. Che was one of the pioneers in the use

of  $^{17}\text{O}$  isotopic labelling in the investigation of catalytic surfaces. [5-7] This was done using  $^{17}\text{O}$  enriched  $\text{O}_2$  in experiments of surface-to-oxygen electron transfer performed to elucidate the mechanisms operating in selective catalytic oxidation. The information achieved was, in those cases, limited to the hyperfine structure of the adsorbed superoxide radical anion in turn related to the structural features of the adsorbed moiety. Much less frequent are however EPR studies involving the incorporation of  $^{17}\text{O}$  at the surface of inorganic oxides,[8-11] a strategy that offers unique opportunities to directly follow the metal-oxide interaction and largely developed by our group.[12-17] In this work we apply a multi-frequency EPR approach and show how  $^{17}\text{O}$  isotopic labelling of a MFI zeolite framework in conjunction with Hyperfine Sublevel Correlation Spectroscopy (HYSCORE) at Q band frequency can provide detailed information on the interaction of isolated  $\text{V}^{4+}$  species prepared by evaporation of  $\text{VCl}_4$  onto H-ZSM5.

V species in porous and microporous materials are one such example. A number of ways exist to incorporate V species on zeolite surfaces, among which the evaporation of molecular precursors such as  $\text{VOCl}_3$  or  $\text{VCl}_4$  are particularly well suited to generate isolated single sites, amenable to detailed spectroscopic studies.[18-20] Here we focus on the characterization of the vanadium support interaction providing the full hyperfine interaction tensor to  $^{17}\text{O}$  framework nuclei. Comparison will be set to molecular aquo vanadyl solvated ions, providing a further link between surface coordinated metal-oxide species and solution coordination chemistry, in the spirit of Michel Che's interfacial coordination chemistry concept.

## Experimental

The H-ZSM-5 zeolite (commercial sample CBV8014, supplied by Zeolyst, Si/Al = 40) was dehydrated by thermal treatment at 673 K under dynamic vacuum (residual pressure  $<10^{-4}$  mbar) for two hours and subsequently calcined at 773 K in  $\text{O}_2$  atmosphere to remove spurious organic residues.

Framework substitution of  $^{16}\text{O}$  by  $^{17}\text{O}$  was obtained by heating the dehydrated H-ZSM5 at 120 °C for 2 h, in presence of  $\text{H}_2^{17}\text{O}$  vapors as described elsewhere [17].

The anhydrous vapour exchange process was performed at room temperature exposing the  $^{17}\text{O}$ -enriched zeolite to the  $\text{VCl}_4$  vapours in a quartz cell equipped with an EPR tube. The cell was evacuated after the reaction to remove excess  $\text{VCl}_4$  and the reaction products (HCl).

X-band (microwave frequency 9.46 GHz) CW EPR spectra were performed on a Bruker EMX spectrometer equipped with a cylindrical cavity. A modulation frequency of 100 kHz, a modulation amplitude of 0.2 mT, and a microwave power of 0.02 mW were used. Q-band (microwave frequency 33.7 GHz) CW-EPR experiments were performed on a Bruker ELEXYS 580 EPR spectrometer, equipped with helium gas-flow cryostat from Oxford Inc. The magnetic field was measured with a Bruker ER035M NMR gaussmeter. W-band experiments (microwave frequency 95 GHz) were performed on a Bruker Elexysis E600 Spectrometer (Cardiff University). For Q and W band

measurements, the samples were introduced in the EPR tubes in a glove box ( $O_2 < 0.5$  ppm,  $H_2O < 0.5$  ppm) and sealed in order to avoid contact with the atmosphere.

Q-band Electron-spin-echo (ESE) detected EPR spectra were recorded with the pulse sequence  $\pi/2-\tau-\pi-\tau$ -echo. Pulse lengths  $t_{\pi/2} = 16$  ns and  $t_{\pi} = 32$  ns, a  $\tau$  value of 200 ns and a 0.5 kHz shot repetition rate were used.

Q-band Hyperfine Sublevel Correlation (HYSCORE) [21] experiments were carried out with the pulse sequence  $\pi/2-\tau-\pi/2-t_1-\pi-t_2-\pi/2-\tau$ -echo, applying a eight-step phase cycle for eliminating unwanted echoes. Microwave pulse lengths  $t_{\pi/2} = 16$  ns,  $t_{\pi} = 32$  ns, and a shot repetition rate of 0.5 kHz were used. The  $t_1$  and  $t_2$  time intervals were incremented in steps of 8 ns, starting from 200 ns giving a data matrix of 250 x 250 points. The time traces of the HYSCORE spectra were baseline corrected with a third-order polynomial, apodized with a Hamming window and zero filled. After two-dimensional Fourier transformation, the absolute value spectra were calculated. Spectra with different  $\tau$  values were recorded, which are specified in the figure captions. The spectra were added for the different  $\tau$  values in order to eliminate blind-spot effects. All EPR spectra were simulated employing the Easyspin package. [22] 170 HYSCORE simulations were performed considering interactions with each of the 170 nuclei separately and the individual simulated HYSCORE spectra were added together. This was done since no combination frequencies were observed in the HYSCORE spectra, excluding the analysis of the relative orientation of the different 170 hyperfine tensors.

## Results and discussion

Accurate  $g$  and  $A^{(51V)}$  tensors (nuclear spin  $I^{(51V)}=7/2$  abundance 99.76%) were extracted from powder EPR spectra through the analysis of CW-EPR spectra recorded at, X (9.5 GHz), Q (34 GHz) and W-band (94 GHz). X-, Q- and W-band spectra were recorded at 77 K, 30 K and 20 K, respectively and are shown in Figure 1 along with the corresponding computer simulations.

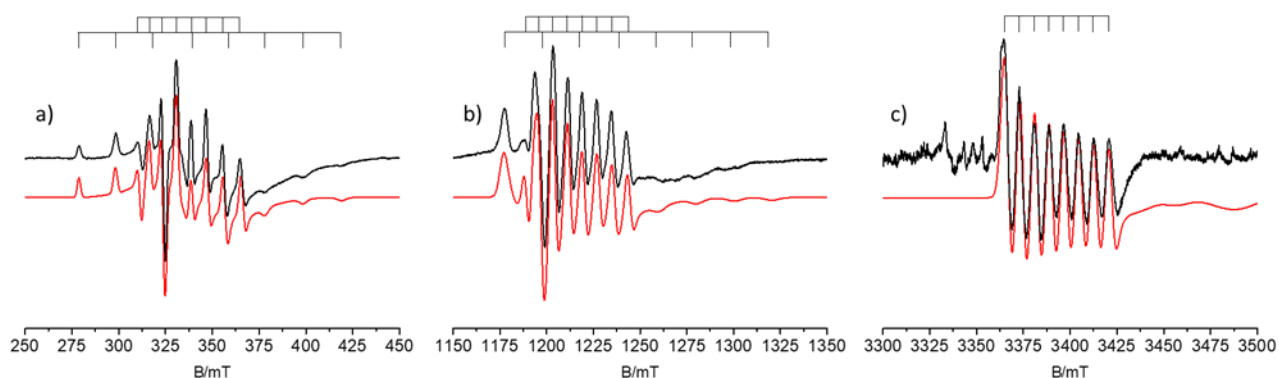


**Figure 1** Experimental (black) and simulated (red) CW-EPR spectra of the V/ZSM-5 sample recorded at a) X-band, b) Q-band and c) W-band frequencies. Due to strain effects, the parallel components of the W-band spectrum are unresolved.

The spectra do not change appreciably in the temperature interval 298K-10K and are characterized by an eight-fold hyperfine splitting of all anisotropic components typical of  $V^{4+}$ , indicating absence of mobility of the grafted species. As typically observed in the case of supported vanadium species, a broad background centred at approximately  $g=1.998$  suggests the presence of  $V^{4+}$  aggregates.[23,24] These contributions disappear in the echo detected EPR spectrum (Figure 2a) as expected for dipolarly interacting species characterized by a short phase memory time ( $T_m$ ). Inspection of spectra recorded at the different frequencies shows a progressive apparent increase in the line width, in particular of the parallel components, associated to a distribution of local  $g$  and  $A$  values (strain) and reflecting a distribution of binding sites with slightly different ligand fields. Spectral simulations were performed at the three frequencies based on the following spin Hamiltonian:

$$\mathcal{H} = \hat{I} \cdot \mathbf{A} \cdot \hat{S} + \mu_B \hat{S} \cdot \mathbf{g} \cdot \mathbf{B} \quad (1)$$

The X-band EPR spectrum could be satisfactorily simulated assuming a collinear axial model (*i.e.*  $x = y \neq z$ , where  $x, y, z$  refer to the principal directions of the  $\mathbf{g}$  and  $\mathbf{A}$  tensors. A small discrepancy in the positions of the hyperfine transitions and line shapes were observed between the X-band and the higher frequencies (Q- and W-band). Therefore, the possibility of a non-collinearity between the  $\mathbf{A}$  and  $\mathbf{g}$  tensor axes, was investigated. When tilting between the  $\mathbf{g}$  and  $\mathbf{A}$  ( $^{51}\text{V}$ ) tensor principal axes of  $6 \pm 2^\circ$  is introduced, the spectra in the three frequency bands are convincingly reproduced using the parameters reported in Table 1.

Sample	Species	$g_x$	$g_y$	$g_z$	$A_x$	$A_y$	$A_z$
V/ZSM5	$\text{VO}^{2+}$	$1.9843 \pm 0.0002$	$1.9843 \pm 0.0002$	$1.931 \pm 0.001$	$ 214 \pm 3 $	$ 214 \pm 3 $	$ 542 \pm 3 $
	aggregate	$1.965 \pm 0.0008$			-	-	-
$\text{VO}(\text{H}_2\text{O})_5^{2+}$	$\text{VO}^{2+}$ [25]	1.978	1.978	1.939	-	-	-
	$\text{VO}^{2+}$ [26,27]	1.978	1.978	1.933	-212	-212	-547
	$\text{VO}^{2+}$ [28]	1.982	1.982	1.936	-210	-210	-534

**Table 1** Spin-Hamiltonian parameters derived from the simulation of the CW EPR spectra. Hyperfine coupling constant values are given in units of MHz.

Given the preparation method, *i.e.* the anhydrous solid-gas phase reaction between HZSM-5 and  $\text{VCl}_4$ , an issue of interest is to understand whether  $V^{4+}$  or vanadyl  $\text{VO}^{2+}$  centres are formed upon reaction. In turn this informs on the inter-atomic distance between the vanadium centre and the nearest neighbor oxygen, which for  $\text{VO}^{2+}$  remains significantly closer to the transition metal ion.

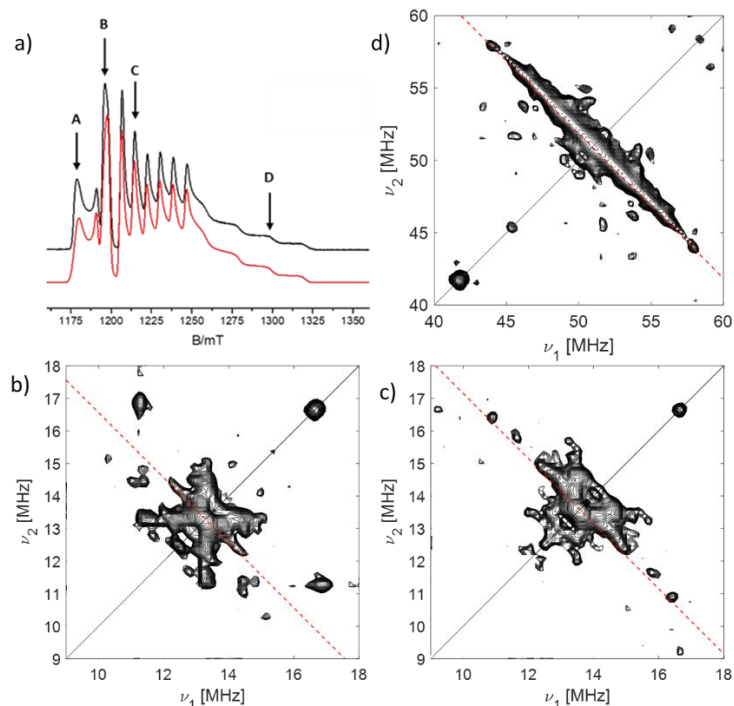


**Figure 2** a) Experimental (black) and simulated (red) Q-band Echo detected EPR spectrum of the V/ZSM5 sample. The spectrum was recorded at 10 K and  $\tau = 200$  ns. The letters indicate the magnetic field settings at which  $^{17}\text{O}$  HYSCORE experiments were carried out; b) Experimental  $^{27}\text{Al}$  Q-Band HYSCORE spectrum recorded at position B ( $B_0 = 1196$  mT) and  $\tau = 110$  ns c)  $^{27}\text{Al}$  Q-Band HYSCORE spectrum recorded at position C ( $B_0 = 1222$  mT) and  $\tau = 110$  ns. The HYSCORE spectra were symmetrized; d)  $^1\text{H}$  Q-Band HYSCORE spectrum recorded at position B ( $B_0 = 1196$  mT). The spectrum is the sum of two spectra recorded at  $\tau = 110$  ns and  $\tau = 140$  ns. The red dotted lines in panels b) and c) indicate the  $^{27}\text{Al}$  Larmor frequency, while in panel d) indicate the  $^1\text{H}$  Larmor frequency. All HYSCORE spectra were recorded at 10K. Due to the low intensity, to better appreciate the full ridge extent the HYSCORE spectra were symmetrized.

The spin-Hamiltonian parameters determined by the analysis of the EPR spectra are directly related to structural information considering that the  $\text{V}^{4+}\text{-O}^{2-}$  bond distance is linked to both  $g$  and  $A$  values. In particular, the pseudo-isotropic parameters  $g_{\text{iso}}$  and  $a_{\text{iso}}$ , which can be determined on the basis of the principal values of the  $\mathbf{g}$  and  $\mathbf{A}$  matrices according to  $g_{\text{iso}} = (g_x + g_y + g_z)/3$  and  $^{51}\text{V}a_{\text{iso}} = (A_x + A_y + A_z)/3$  have been proposed to provide an empirical way to discriminate between  $\text{V}^{4+}$  or vanadyl  $\text{VO}^{2+}$  centers. [29] From the spin-Hamiltonian parameters reported in Table 1 we find  $g_{\text{iso}} = 1.9665$  and  $^{51}\text{V}a_{\text{iso}} = 323$  MHz, which falls well within typical values characteristic of  $\text{VO}^{2+}$  species. This analysis thus suggests that the reaction of  $\text{VCl}_4$  with the zeolite results in the formation of  $\text{V}^{4+}\text{-O}^{2-}$  species, featuring a shorter V-O bond with typical characteristics of a vanadyl species. In order to derive a more detailed description of the local environment of the  $\text{V}^{4+}$  centres, orientationally selective Q-band HYSCORE experiments were carried out.

HYSCORE is a two-dimensional experiment where correlation of nuclear frequencies in one electron spin ( $m_s$ ) manifold to nuclear frequencies in the other manifold is created by means of a mixing  $\pi$  pulse, allowing the direct measurement of NMR transitions of magnetically active nuclei coupled to electron spin. The HYSCORE spectra of the V/ZSM-5 unlabeled sample are shown in Figure 2b-d.

The spectra show signals centered at the nuclear Larmor frequencies of  $^{27}\text{Al}$  (Figures 2b,c) and  $^1\text{H}$  (Figure 2d). The  $^{27}\text{Al}$  HYSCORE spectra shows a ridge like pattern with maximum extension of the order of 2.5 MHz. The ridge shape and vertical displacement from the  $\nu_1 = -\nu_2$  axis indicates that the interaction has a significant dipolar contribution. For electron-nuclear distances,  $r$ , larger than 0.25 nm, and for negligible spin delocalization over the ligand the dipolar approximation holds:

$$T = \frac{\mu_0}{4\pi} g_e g_n \beta_e \beta_n \frac{1}{r^3} \quad (3)$$

with  $r$  being the distance between the unpaired electron localized in the V  $d$  orbitals and the nucleus  $n$ . Due to the low spectral intensity, a proper orientation selective analysis was not possible, however fitting of the spectra recorded at two different observer positions, confirm this analysis, indicating a dipolar coupling  $^{\text{Al}}T \approx 0.95$  MHz and the approximate collinearity of the  $g_z$  and  $^{\text{Al}}T_z$  axes. Similar values, although slightly higher, were reported in the case of vanadyl species located in aluminum phosphate materials and can be considered indicative of the interaction of the unpaired electron on the V ion with aluminum framework atoms in the second coordination shell. [30,31] Assuming a negligible  $a_{\text{iso}}$  value, the distance  $r_{\text{V-Al}} \approx 0.28 \pm 0.03$  nm between the  $\text{VO}^{2+}$  ion and a framework Al ion is derived, using the point dipole approximation. This value is in fair agreement with the V-Al distance reported by Iglesia on a V/ZSM-5 exchanged zeolite via reaction with gas phase  $\text{VOCl}_3$  [18]

Centered at the  $^1\text{H}$  Larmor frequency, a pronounced ridge with a maximum width of about 13 MHz is also observed (Figure 2d). The ridge can be simulated using values reported in previous studies concerning vanadyl species on the surface of silicate [32] or aluminophosphate [31] systems ( $a_{\text{iso}} = 3.5 \pm 0.5$  MHz  $T = 4.5 \pm 0.5$  MHz) and coherent with data based on quantum chemical calculations [33] and single crystal ENDOR [26] experiments for equatorially bound hydroxyls of  $[\text{VO}(\text{H}_2\text{O})_5]^{2+}$ . Considering a purely dipolar interaction the V-H distance can be estimated using Equation 3 to be  $r_{\text{V-H}} = 0.26 \pm 0.01$  nm. Interestingly no evidence was found for coordinating Cl nuclei, suggesting a complete hydrolysis of the  $\text{VCl}_4$  molecules by reaction with surface OH groups and  $\text{H}_2\text{O}$  molecules. CW EPR and HYSCORE measurements on the unlabeled V/ZSM-5 sample have demonstrated the formation of a short  $\text{V}^{4+}$ -O bond characteristic of a  $\text{VO}^{2+}$  species and well-defined interactions with  $^{27}\text{Al}$  framework ions and protons located in the second coordination sphere. Although well-detailed, these data are not sufficient for a full description of the local coordinating environment, that can only be obtained through the detection of hyperfine interactions to  $^{17}\text{O}$  framework nuclei in the  $^{17}\text{O}$  exchanged zeolite.

The  $^{17}\text{O}$  HYSCORE spectrum recorded at a magnetic field setting corresponding to position B in Figure 2a ( $B_0 = 1996$  mT) is shown in Figure 3, along with its computer simulation.

The spectrum is dominated by the presence of two off-diagonal cross peaks at about (9.5, 4.5) MHz and (4.5, 9.5) MHz, centered at the  $^{17}\text{O}$  Larmor frequency  $\nu_0 = 6.9$  MHz and relating the  $m_1 \frac{1}{2} \rightarrow -\frac{1}{2}$  transitions of the two  $m_s$  manifolds (single quantum transitions, SQ-SQ). Additional, cross peaks at (19, 4.5) MHz and (4.5, 19) MHz, and (19, 9) MHz and (9, 19) MHz, shown in the inset of Figure 3,



are assigned to single-double (SQ-DQ) and double quantum (DQ-DQ) transitions. Due to the lower transition probability, these cross peaks have lower intensities and are therefore plotted separately in the inset, at a higher contour level. Inspection of Figure 3 shows that the moderately elongated SQ cross peaks are composed by a central, intense peak, flanked by two extra cross peaks with lower intensity. These cross peaks can be rationalized as being part of a splitting quintet due to the nuclear quadrupole interaction. The considerable larger intensity of the central cross peaks with respect to the satellite lines suggests the presence of two set of nuclei, one with a small nuclear quadrupole value (contributing to the central line, hereafter termed O1), the other with a larger coupling responsible for the splitting structure (thereafter referred to as O2). This was confirmed by a simulation analysis, which proved impossible to convincingly fit the spectrum with a single set of nuclei, reproducing both the splitting and the relative intensity of the different cross peaks.

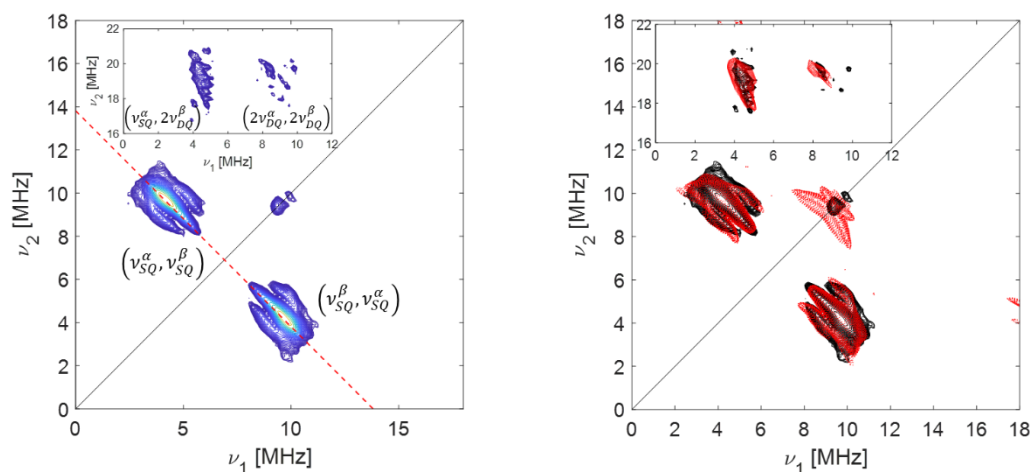


**Figure 3** Experimental and simulated (red)  $^{17}\text{O}$  HYSCORE spectra of a  $^{17}\text{O}$  enriched V/ZSM-5 sample. The spectra are recorded at a magnetic field setting  $B_0=1996$  mT with  $\tau=144$  ns at 10 K. The simulation is obtained by summing the contributions of two O nuclei (O1 and O2 in table 2) after Fourier transform. The contour level of the simulation was set in order to match the intensity of the experimental spectrum. The dotted red line indicates the  $^{17}\text{O}$  Larmor frequency.

In the limit of a small quadrupole interaction, the  $^{17}\text{O}$  cross peaks will be centered at  $\nu = \nu_1 \pm A/2$ , where  $\nu_1$  is the  $^{17}\text{O}$  nuclear Larmor frequency. From the simulation of the HYSCORE spectra recorded at different magnetic field settings, the central intense pair of cross peak belonging to O2 could be simulated with the parameters reported in Table 2. From these values a Fermi contact ( $a_{\text{iso}}$ ) term of about 4 MHz and an anisotropic coupling tensor  $T = [-1.7 \pm 0.5 \ -1.7 \pm 0.5 \ +3.4 \pm 0.5]$  MHz are extracted. The derived  $^{17}\text{O}$  hyperfine interaction is nearly one order of magnitude smaller than the one observed for  $\text{Zn}^+$  ions featuring a  $4s^1$  ground state [17] and reflects the non-bonding character of the  $d_{xy}$  orbital hosting the unpaired electron and concurs with values reported for pentaquo vanadyl molecular complexes.[25, 34] The dipolar hyperfine tensor translate into a V-O1 distance of the order of 0.19 nm. This value correlates with V-O distances determined by EXAFS experiments for  $\text{VO}^{2+}$  in ZSM-5 obtained by hydrolysis of  $\text{VOCl}_3$ . Such experiments revealed more than one class of oxo-ions around V with distances ranging between 0.18 nm and 0.20 nm as well as the short V=O bond

at about 0.16 nm [18]. The orientation of the  $\mathbf{T}$  tensor relative to the  $\mathbf{g}$  tensor principal frame, given by the Euler angle  $\beta$ , shows that the V-O2 bond forms is tilted by  $\approx 50^\circ$  with respect to the  $g_z$  axis which, in the case of a vanadyl ion, is assumed to be collinear with the direction of the shortest V=O bond. Hence, the hyperfine parameters point to a geometry where the O=V-O2 angle is of the order of  $130^\circ$  (Scheme 1). Spectral simulations allow to estimate the upper limit of the nuclear quadrupole interaction for O2 as  $e^2qQ/h = 2 \pm 0.5$  MHz.

The splitting lines observed in the experimental spectrum are due to the nuclear quadrupole interaction of O1 and can be reproduced with  $e^2qQ/h$  values of the order of  $9 \pm 1$  MHz, keeping the hyperfine parameters ( $a_{\text{iso}}$  and  $T$ ) unchanged. This value is in line with the value of 10.7 MHz reported by Baute and Goldfarb [25] for equatorially bound  $^{17}\text{O}$  labelled water molecules in the vanadyl aquo complex. The result of this simulation approach is shown in Figure 3 where the computer simulation (red) is superimposed on the experimental spectrum (black) for the easy of comparison.

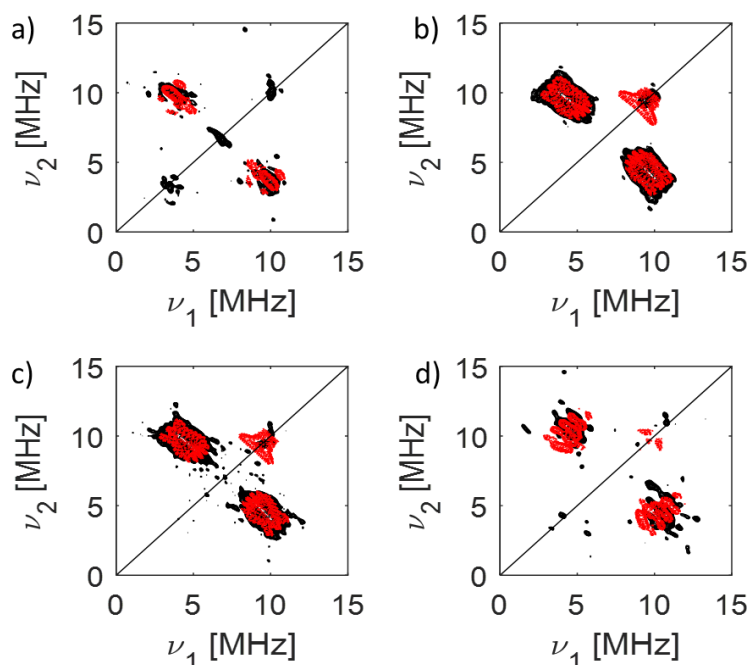


**Figure 4** Experimental (black) and simulated (red)  $^{17}\text{O}$  HYSCORE spectra of the  $\text{VCl}_4$ -ZSM5 sample. a) observer position:  $B_0=1180.7$  mT  $\tau=216$  ns; b) observer position:  $B_0=1196.0$  mT,  $\tau=144$  ns; c) observer position  $B_0=1213.1$  mT  $\tau=144$  ns and (d) observer position:  $B_0=1300.0$  mT,  $\tau=144$  ns. All spectra were recorded at  $T=30$  K. The contour level of the simulations as adjusted to the intensity of the experimental spectra.

The simulation correctly reproduces the relevant features, including the single-double and double quantum transitions (see inset in Figure 3). The same set of parameters was then used to simulate the HYSCORE spectra recorded at different magnetic field settings (Figure 4), providing a convincing fit at all fields. The presence of two set of O nuclei, displaying different nuclear quadrupole couplings is a strong indication of different V-O bonds in the system.

$^{17}\text{O}$  hyperfine and quadrupole couplings have been reported for the pentaquo  $\text{V}^{17}\text{O}$  complex by Baute and Goldfarb [25] and later by Cox et al. [34]. In these studies, different  $^{17}\text{O}$  signals were observed,

which were assigned to the different coordinated oxygens based on DFT modelling. A signal with large isotropic and anisotropic hyperfine couplings and a relatively small nuclear quadrupole interaction ( $e^2qQ/h = 3.5$  MHz) was assigned to the oxo ligand, while a signal with large  $a_{\text{iso}}$ , small anisotropic hyperfine coupling and large nuclear quadrupole interaction was assigned to equatorially bound water. **[Errore. Il segnalibro non è definito.]** A third signal, with intermediate values was reported by Cox and tentatively assigned to axially coordinated water molecules, although the Authors did not exclude a second type of equatorial water ligand.

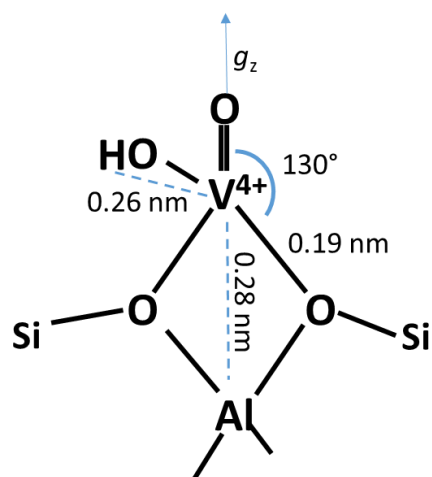
In the case of the surface bound vanadyl, the signal characterized by a large nuclear quadrupole (O1 in Table 2), fits well with the signal of coordinated water molecules and can be assigned to coordinated hydroxyl species consistent with the observation of a proton coupling. The other oxygen (O2 in Table 2), characterized by similar hyperfine couplings but a lower quadrupole interaction, can be assigned to oxygen framework ions to which the surface vanadyl species is anchored. For such framework oxygens low  $^{17}\text{O}$  quadrupole values were recently reported by us in the case of open-shell  $\text{Zn}^+$  ions bound at a  $^{17}\text{O}$  enriched ZSM-5 zeolite framework. [17] Despite the evidence coming from the V spin Hamiltonian parameters of a V=O bond, the  $^{17}\text{O}$  HYSCORE spectra show no evidence for the typical  $^{17}\text{O}$  signal with large dipolar couplings characteristic of the oxo ligand. This signal was clearly observed in W-band Davies ENDOR [25] and W-band EDNMR spectra. **[Errore. Il segnalibro non è definito.]** Failure to observe such signal in Q-band HYSCORE experiments may be due to suppression effects associated to the presence of more than one nucleus coupled to the electron spin.[35]

Sample	Nuclei	$A_x$	$A_y$	$A_z$	Euler angle $\alpha, \beta, \gamma$	$e^2qQ/h$	$\eta$	Euler angle $\alpha', \beta', \gamma'$
V/ZSM5	$^{17}\text{O}(1)$	$2.6 \pm 0.5$	$2.6 \pm 0.5$	$7.2 \pm 0.5$	0, $60 \pm 10$ , 0	$9.5 \pm 0.5$	$0.2 \pm 0.2$	0, $70 \pm 10$ , 0
	$^{17}\text{O}(2)$	$2.6 \pm 0.5$	$2.6 \pm 0.5$	$7.2 \pm 0.5$	0, $50 \pm 10$ , 0	$2.0 \pm 0.5$	0.0	
	$^{27}\text{Al}$	$-0.35 \pm 0.5$	-	$2.5 \pm 0.5$	0, $0 \pm 20$ , 0	n. d.		
	$^1\text{H}$	$-1.0 \pm 0.5$	$-1.0 \pm 0.5$	$12.5 \pm 0.5$	0, $60 \pm 20$ , 0			
$\text{VO}(\text{H}_2\text{O})_5^{2+}$ [25]	$^{17}\text{O}(\text{oxo})$	16	16	-6.9	0, 0, 0	3.3	0.14	0, 0, 0
	$^{17}\text{O}(\text{eq.})$	8	6.3	7.2	x, 0, 0	10.7	0.52	0, 0, 0
$\text{VO}(\text{H}_2\text{O})_5^{2+}$	$^{17}\text{O}(\text{oxo})$	15.8	15.8	4.4		3.3	0.14	
	$^{17}\text{O}(\text{eq.})$	8.8	5.4	7.1		10.7	0.52	
	$^{17}\text{O}(\text{ax.})$	3.8	3.3	7.9		10.7	0.52	

**Table 2** Spin Hamiltonian parameters derived from the simulation of the HYSCORE experiments

To summarize, the analysis of multifrequency EPR experiments of vanadyl species, introduced in H-ZSM-5 through reaction of the zeolite with  $\text{VCl}_4$  vapours, provides evidence for the formation of isolated vanadyl species. HYSCORE experiments indicate the interaction of such vanadyl species

with at least one Al ion in the second coordination sphere at a distance of the order of 0.28 nm and a directly linked hydroxyl species with a H-V distance of the order of 0.26 nm. Moreover,  $^{17}\text{O}$  HYSCORE experiments indicate the presence of at least two different binding oxygens characterized by different nuclear quadrupole couplings and assigned to the hydroxyl oxygen (large coupling) and a framework oxygen ion (low quadrupole). These results indicate that the grafting protocols place V-oxo species onto the exchange site featuring Al species, with an all-oxygen first coordination sphere. The lack of Cl couplings is understood as the result of consecutive hydrolysis steps involving surface hydroxyls and residual water molecules, which are still present in the zeolite channels after the exchange treatment. A similar reaction path was reported by Lacheen and Iglesia [20] for the reaction of gas phase  $\text{ZrCl}_4$  with H-ZSM-5 and subsequent hydrolysis. Reaction of  $\text{ZrCl}_4$  with acidic OH groups was proven to lead to  $\text{HCl}$  and  $\text{ZrCl}_3^+$ -ZSM5 species, which evolved during hydrolysis, into  $\text{ZrO}(\text{OH})^+$  species. This reaction pathway nicely agrees with our observation of vanadyl species coordinated to a hydroxyl ion and the absence of coordinating Cl ions. Charge neutralities requires that such species, featuring a single positive charge, are localized at Al sites as shown in Scheme 1, whereby they compensate for the proton charge. In this scheme the Al ion is located along the direction of the  $\text{V}=\text{O}$  bond, coinciding with the  $g_z$  component of the  $\mathbf{g}$  tensor and below the xy plane, where the spin density is located ( $d_{xy}$  orbital). This geometrical arrangement is consistent with T7 sites sitting at the zeolite channels intersection and with the low spin density transfer to the Al ion and a distance Al-V of the order of 0.28 nm, consistent with Zn-Al distances observed at similar sites [17]. The  $\text{O}=\text{V}-\text{O}$  angle can be derived from the orientation of O(2) with respect to the  $g_z$  component leading to a bond angle of  $130^\circ \pm 10^\circ$  consistent with  $\text{VO}^{2+}$  units coordinated at the surface of heteropolyacids, [36] We remark that this coordination geometry does not exclude the possible binding at other sites such as T8, placed on the wall of the straight channel, with a relatively flat local environment and potentially favouring coordination to a larger number of oxygens. The possibility that OH free  $\text{V}=\text{O}$  species, resulting from the condensation of two monomers, are present cannot be excluded, but such species will require sites featuring two neighbouring Al ions to compensate for the +2 charge as shown in structure 2. Clearly, the abundance of such species will depend on the Al/Si ratio.



## Scheme 1

Moreover, monomeric  $\text{VO}(\text{OH})^+$  could de-anchor in the presence of trace moisture to exchange and migrate possibly to external surfaces and form aggregates, which may explain the broad background observed in the CW EPR spectra.

## Conclusion

$\text{V}^{4+}$  cations were grafted selectively onto Al sites in H-ZSM5 using  $\text{VCl}_4$  vapor under anhydrous conditions. A combination of CW and pulse EPR experiments at different frequencies provide evidence for the formation of  $\text{VO}^{2+}$  species upon hydrolysis of the molecular precursor with surface OH Structures and residual water molecules, leading to the complete dechlorination of the V species and formation of monomeric  $\text{VO}(\text{OH})^+$  species. A combination  $^1\text{H}$ ,  $^{27}\text{Al}$  and  $^{17}\text{O}$  HYSCORE experiments at Q band frequency, allows recovering the full set of hyperfine tensors related to the first and second coordination sphere of the vanadium ion allowing for a detailed geometrical description of the structure of the isolated single metal sites. Analysis of the  $^{17}\text{O}$  hyperfine interaction, shows that the monomeric vanadyl species bear resemblance to solvated species in solution, reinforcing the notion of the zeolite framework as a macroligand and allowing for a detailed description of the geometrical and electronic structure of the surface anchored species. Moreover, this methodological approach is of general applicability, showing that advanced EPR methodologies combined with isotopic enrichment, can be of high relevance in interrogating heterogeneous systems of catalytic relevance, providing detailed answers on specific question related to the structure and function of open-shell sites.

## Acknowledgment

## References

- 
- [1] M. Che, Interfacial Coordination Chemistry: Concepts and Relevance to Catalysis Phenomena, *Stud. Surf. Sci. Catal.* 75 (1993) 31-68.
  - [2] K. Dyrek, M. Che, EPR as a Tool To Investigate the Transition Metal Chemistry on Oxide Surfaces, *Chem. Rev.* 97 (1997) 305-332.
  - [3] Z. Sojka, Molecular Aspects of Catalytic Reactivity. Application of EPR Spectroscopy to Studies of the Mechanism of Heterogeneous Catalytic Reactions, *Catal. Rev.* 37 (1995) 461-512.
  - [4] S. E. Ashbrook, M. E. Smith, Solid state  $^{17}\text{O}$  NMR—an introduction to the background principles and applications to inorganic materials, *Chem. Soc. Rev.* 35 (2006) 718–735.
  - [5] M. Che, A. J. Tench, Characterization and Reactivity of Mononuclear Oxygen Species on Oxide Surfaces, *Adv. Catal.* 31 (1982) 77-133.
  - [6] M. Che, A. J. Tench, Characterization and Reactivity of Molecular Oxygen Species on Oxide Surfaces, *Adv. Catal.* 32 (1983) 1-148.
  - [7] M. Che, E. Giamello, A. J. Tench, The role of the  $^{17}\text{O}$  isotope in the characterisation by EPR of adsorbed oxygen species on oxide surfaces, *Colloids Surf.* 13 (1985) 231-248.
  - [8] N. B. Wong, J. H. Lunsford, EPR Study of  $^{17}\text{O}^-$  on Magnesium Oxide, *J. Chem. Phys.* 55 (1971) 3007-3012.

- 
- [9] O. I. Micic, Y. Zhang, K. R. Cromack, A. D. Trifunac, M. C. Thurnauer, Trapped holes on titania colloids studied by electron paramagnetic resonance, *J. Phys. Chem.* 97 (1993) 28 7277-7283.
- [10] V. Brezová, Z. Barbieriková, M. Zukalová, D. Dvoranová, L. Kavan, EPR study of  $^{17}\text{O}$ -enriched titania nanopowders under UV irradiation, *Catal. Today* 230 (2014) 112-118.
- [11] F. Wang, R. Büchel, A. Savitsky, M. Zalibera, D. Widmann, S. E. Pratsinis, W. Lubitz, F. Schüth, In Situ EPR Study of the Redox Properties of CuO–CeO<sub>2</sub> Catalysts for Preferential CO Oxidation (PROX), *ACS Catal.* 6 (2016) 3520–3530.
- [12] M. Chiesa, P. Martino, E. Giamello, C. Di Valentin, A. del Vitto, G. Pacchioni, Local Environment of Electrons Trapped at the MgO Surface: Spin Density on the Oxygen Ions from  $^{17}\text{O}$  Hyperfine Coupling Constants, *J. Phys. Chem. B* 108 (2004) 11529-11534.
- [13] M. Chiesa, E. Giamello, C. Di Valentin, G. Pacchioni, The  $^{17}\text{O}$  hyperfine structure of trapped holes photo generated at the surface of polycrystalline MgO, *Chem. Phys. Lett.* 403 (2005) 124-128.
- [14] M. Chiesa, E. Giamello, C. Di Valentin, G. Pacchioni, Z. Sojka, S. Van Doorslaer, Nature of the Chemical Bond between Metal Atoms and Oxide Surfaces: New Evidences from Spin Density Studies of K Atoms on Alkaline Earth Oxides, *J. Am. Chem. Soc.* 127 (2005) 16935–16944.
- [15] S. Livraghi, S. Maurelli, M. C. Paganini, M. Chiesa, E. Giamello, Probing the Local Environment of Ti<sup>3+</sup> Ions in TiO<sub>2</sub> (Rutile) by  $^{17}\text{O}$  HYSCORE, *Angew. Chem. Int. Ed.* 50 (2011) 8038-8040.
- [16] S. Livraghi, M. Chiesa, M. C. Paganini, E. Giamello, On the Nature of Reduced States in Titanium Dioxide As Monitored by Electron Paramagnetic Resonance. I: The Anatase Case, *J. Phys. Chem. C* 115 (2011) 25413-25421.
- [17] E. Morra, M. Signorile, E. Salvadori, S. Bordiga, E. Giamello, M. Chiesa, Nature and Topology of Metal–Oxygen Binding Sites in Zeolite Materials:  $^{17}\text{O}$  High-Resolution EPR Spectroscopy of Metal-Loaded ZSM-5, *Angew. Chem.* 131 (2019) 12528 –12533.
- [18] B. I. Whittington, J. R. Anderson Vanadium-Containing ZSM5 Zeolites: Reaction between Vanadyl Trichloride and ZSM S/IIIcalle J. Phys. Chem. 95 (1991) 3306-3310
- [19] H. S. Lacheen, E. Iglesia Synthesis, Structure, and Catalytic Reactivity of Isolated V<sup>5+</sup>-Oxo Species Prepared by Sublimation of VOCl<sub>3</sub> onto H-ZSM5, *J. Phys. Chem. B* 110 (2006) 5462-5472.
- [20] H. S. Lacheen, E. Iglesia, Structure of Zirconium-Exchanged H-ZSM5 Prepared by Vapor Exchange of ZrCl<sub>4</sub>, *Chem. Mater.* 19 (2007) 1877-1882.
- [21] P. Höfer, A. Grupp, H. Nebenführ, M. Mehring, Hyperfine sublevel correlation (hyscore) spectroscopy: a 2D ESR investigation of the squaric acid radical, *Chem. Phys. Lett.* 132 (1986) 279-282.
- [22] S. Stoll, A. Schweiger, EasySpin, a comprehensive software package for spectral simulation and analysis in EPR, *J. Magn. Reson.* 178 (2006) 42-55.
- [23] Z. Luan, L. Kevan, Electron Spin Resonance and Diffuse Reflectance Ultraviolet–Visible Spectroscopies of Vanadium Immobilized at Surface Titanium Centers of Titanosilicate Mesoporous TiMCM-41 Molecular Sieves, *J. Phys. Chem.* 101 (1997) 2020-2027.
- [24] M. Baltes, K. Cassiers, P. Van Der Voort, B. M. Weckhuysen, R. A. Schoonheydt, E. F. Vansant, MCM-48-Supported Vanadium Oxide Catalysts, Prepared by the Molecular Designed Dispersion of VO(acac)<sub>2</sub>: A Detailed Study of the Highly Reactive MCM-48 Surface and the Structure and Activity of the Deposited VO<sub>x</sub>, *J. Catal.* 197 (2001) 160-171.
- [25] D. Baute, D. Goldfarb, The  $^{17}\text{O}$  Hyperfine Interaction in V<sup>17</sup>O(H<sub>2</sub><sup>17</sup>O)<sub>5</sub><sup>2+</sup> and Mn(H<sub>2</sub><sup>17</sup>O)<sub>6</sub><sup>2+</sup> Determined by high Field ENDOR Aided by DFT Calculations, *J. Phys. Chem. A* 109 (2005) 7865-7871.
- [26] N. M. Atherton, J. F. Shackleton, Proton ENDOR of VO(H<sub>2</sub>O)<sub>5</sub><sup>2+</sup> in Mg(NH<sub>4</sub>)<sub>2</sub>(SO<sub>4</sub>)<sub>2</sub>·6H<sub>2</sub>O, *Mol. Phys.* 39 (1980) 1471-1485.
- [27] N. D. Chasteen, Vanadyl(IV) EPR Spin Probes Inorganic and Biochemical Aspects, in: L. J. Berliner, J. Reuben (Eds.) *Biological Magnetic Resonance*, Plenum Press, New York, 1981, Vol. 3, p 53-119.
- [28] G. Martini, M. F. Ottaviani, G. L. Seravalli, Electron spin resonance study of vanadyl complexes adsorbed on synthetic zeolites, *J. Phys. Chem.* 1975, 79, 1716-1720.
- [29] P. Jakes, R.-A. Eichel, Characterization of tetravalent vanadium functional centres in metal oxides derived from a spin-Hamiltonian analysis, *Mol. Phys.* 110 (2012) 277-282.
- [30] V. Nagarajan, D. Rings, L. Moschkowitz, M. Hartmann, A. Pöpl, Location of Vanadium(IV) in VAPO-5 as Studied by Hyperfine Sublevel Correlation Spectroscopy, *Chem. Lett.* 34 (2005) 1614-1615.

- 
- [31] S. Maurelli, G. Berlier, M. Chiesa, F. Musso, F. Corà, Structure of the Catalytic Active Sites in Vanadium-Doped Aluminophosphate Microporous Materials. New Evidence from Spin Density Studies, *J. Phys. Chem. C* 118 (2014) 19879–19888.
- [32] M. Chiesa, V. Meynen, S. Van Doorslaer, P. Cool, E. F. Vansant, Vanadium Silicalite-1 Nanoparticles Deposition onto the Mesoporous Walls of SBA-15. Mechanistic Insights from a Combined EPR and Raman Study, *J. Am. Chem. Soc.* 128 (2006) 8955-8963.
- [33] S. C. Larsen, DFT Calculations of Proton Hyperfine Coupling Constants for  $[\text{VO}(\text{H}_2\text{O})_5]^{2+}$ : Comparison with Proton ENDOR Data, *J. Phys. Chem. A.* 105 (2001) 8333-8338.
- [34] N. Cox, W. Lubitz, A. Savitsky W-band ELDOR-detected NMR (EDNMR) spectroscopy as a versatile technique for the characterisation of transition metal–ligand interactions, *Mol. Phys.* 111 (2013), 2788-2808
- [35] S. Stoll, C. Calle, G. Mitrikas, A. Schweiger Peak suppression in ESEEM spectra of multinuclear spin systems *J. Mag. Reson.* 177, (2005) 93-101.
- [36] A. Poepl, P. Manikandan, K. Koehler, P. Maas, P. Strauch, R. Boettcher, D. Goldfarb, Elucidation of Structure and Location of V(IV) Ions in Heteropolyacid Catalysts  $\text{H}_4\text{PVMo}_{11}\text{O}_{40}$  as Studied by Hyperfine Sublevel Correlation Spectroscopy and Pulsed Electron Nuclear Double Resonance at W- and X-Band Frequencies, *J. Am. Chem. Soc.* 123 (2001) 4577-4584.